



Contents lists available at ScienceDirect

Leukemia Research

journal homepage: www.elsevier.com/locate/leukres



Imatinib does not induce cardiotoxicity at clinically relevant concentrations in preclinical studies

Armin Wolf^a, Philippe Couttet^a, Min Dong^a, Olivier Grenet^a, Marcia Heron^b, Ursula Junker^a, Ulrich Laengle^a, David Ledieu^a, Estelle Marrer^a, Anja Nusscher^a, Elke Persohn^a, Francois Pognan^a, Gilles-Jacques Rivière^c, Daniel Robert Roth^a, Christian Trendelenburg^a, Jeffrey Tsao^d, Danielle Roman^{a,*}

^a Preclinical Safety, Novartis Institutes for Biomedical Research, CH-4009 Basel, Switzerland

^b Cardiovascular Physiology, Novartis Institutes for Biomedical Research, Cambridge, MA, USA

^c Drug Metabolism and Pharmacokinetics, Novartis Institutes for Biomedical Research, Basel, Switzerland

^d Global Imaging Group, Novartis Institutes for Biomedical Research, Cambridge, MA, USA

ARTICLE INFO

Article history:

Received 9 October 2009

Received in revised form 2 January 2010

Accepted 5 January 2010

Available online xxx

Keywords:

Imatinib

Cardiotoxicity

c-Abl

Cardiomyocytes

Fibroblasts

siRNA knock down

ABSTRACT

Cytotoxic concentrations of imatinib mesylate (10–50 μ M) were required to trigger markers of apoptosis and endoplasmic reticulum stress response in neonatal rat ventricular myocytes and fibroblasts, with no significant differences observed between c-Abl silenced and nonsilenced cells. In mice, oral or intraperitoneal imatinib treatment did not induce cardiovascular pathology or heart failure. In rats, high doses of oral imatinib did result in some cardiac hypertrophy. Multi-organ toxicities may have increased the cardiac workload and contributed to the cardiac hypertrophy observed in rats only. These data suggest that imatinib is not cardiotoxic at clinically relevant concentrations (5 μ M).

© 2010 Elsevier Ltd. All rights reserved.

1. Introduction

Chronic myeloid leukemia (CML) is a clonal myeloproliferative disorder characterized by the aberrant expansion of hematopoietic cells. The vast majority of patients with CML possess the Philadelphia chromosome [1], a translocation of chromosomes that joins the N-terminus of the *BCR* (breakpoint cluster region) gene on chromosome 22 with the C-terminus of the *ABL* gene (c-Abl) on chromosome 9 [2]. Upon joining, the novel fusion oncogene *BCR-ABL* is formed, which encodes for a constitutively active protein tyrosine kinase [3,4].

Imatinib (Glivec®/Gleevec®) is a small-molecule protein tyrosine kinase inhibitor that potentially inhibits the activity of BCR-ABL, as well as Discoidin Domain Receptor 1 and 2 [5], c-Kit and platelet-derived growth factor receptor- α and - β [6]. Currently, imatinib is approved as a frontline therapy for patients in chronic phase CML, and for patients with CML in all phases (chronic phase, accelerated phase, or blast crisis) following failure of interferon- α therapy [7]. Imatinib therapy has dramatically improved outcomes in CML; imatinib is well tolerated and no cardiotoxic events were identified during development [8–10].

It has been reported that imatinib-treated mice can develop left ventricular (LV) contractile dysfunction and myopathy, and that imatinib induces cell death in isolated cardiomyocytes [11]. It was concluded from those studies that mitochondria played a central role in the imatinib-mediated effects and that the cardiotoxicity was an unanticipated adverse effect of c-Abl inhibition by imatinib. In the present work, those nonclinical imatinib cardiac findings were further assessed in various *in vitro* and *in vivo* studies. The *in vitro* cultured neonatal rat ventricular myocyte (NRVM) model system was used to explore the dose-response relationship of imatinib-induced mitochondrial effects, endoplasmic reticulum (ER) stress, and cytotoxicity to cardiomyocytes. The

Abbreviations: ADP, adenosine diphosphate; ATP, adenosine triphosphate; AUC, area under the concentration–time curve; C_{max} , maximal concentration; c-Abl, C-terminus of Abl gene; CML, chronic myeloid leukemia; ED, end-diastole; ER, endoplasmic reticulum; ES, end-systole; FBS, fetal bovine serum; ip, intraperitoneal; LDH, lactate dehydrogenase; LV, left ventricular; MTS, 3-(4,5-dimethylthiazol-2-yl)-5-(3-carboxymethoxyphenyl)-2-(4-sulfophenyl)-2H-tetrazolium inner salt; NRVM, neonatal rat ventricular myocyte; og, oral gavage; PBS, phosphate buffered saline; T_{max} , time to maximal concentration.

* Corresponding author. Tel.: +41 61 324 10 33; fax: +41 61 696 02 10.

E-mail address: danielle.roman@novartis.com (D. Roman).

cell-type specificity of imatinib-induced cytotoxicity was probed by examining several organ-specific rat fibroblasts compared to NRVMs. The involvement of c-Abl in imatinib-mediated toxicity was evaluated by siRNA knockdown of the c-Abl gene in NRVMs. Finally, exploratory studies in mice (via oral gavage [og], feed-administration or intraperitoneal [ip] administration) and rats (og) were performed to investigate the potential cardiotoxicity of imatinib *in vivo*.

2. Materials and methods

2.1. *In vitro* cultures

Cardiomyocytes were isolated from postnatal days 0–2 Sprague–Dawley rats (RCC, Itingen, Switzerland) using the Neonatal Cardiomyocyte Isolation System (Worthington Biochemical Corporation, Lakewood, NJ, USA) according to the method of Toraason et al. [12]. Briefly, minced ventricular tissue was incubated overnight with trypsin (100 U/mL) at 4 °C. Cells were then pre-plated for 2 h to reduce the presence of fibroblasts in the cultures. During the initial plating, fibroblasts adhere, while myocytes remain in suspension. Nonadherent NRVMs were isolated from suspension and plated at 0.15×10^6 cells/cm² in DMEM/F12 supplemented with 2% fetal bovine serum (FBS), 2% horse serum, 10 U/mL penicillin, 10 µg/mL streptomycin, 100 µM BrdU, 75 µg/mL endothelial cell growth supplement, 10 µg/mL insulin, 5.5 µg/mL transferrin, and 5 ng/mL sodium selenite. NRVMs were cultured at 37 °C, 5% CO₂, and 98% relative humidity. After 48 h, NRVMs exhibited regular spontaneous contractions. Drug treatments started after an additional 2 days of culture. Alternately, the adherent heart fibroblasts were cultured in DMEM/F12 supplemented with 10% FBS, 1% NaHCO₃, 1% Primocin™ (InvivoGen, San Diego, CA), and 1% insulin–transferrin–sodium selenite-X. After four passages, heart fibroblasts were seeded at 0.06×10^6 cells/cm² and used for drug treatments after 24 h in culture.

Rat lung and skin fibroblasts were obtained from the American Type Culture Collection (Manassas, VA, USA) at passage 12+. Lung fibroblasts were subcultured in Ham's F12K with 20% FBS, 100 U/mL penicillin, and 50 µg/mL streptomycin. Skin fibroblasts were subcultured in Eagle's minimum essential medium with 10% FBS, 2 mM L-glutamine, 1% non-essential amino acids, 1 mM sodium pyruvate, 100 U/mL penicillin, and 50 µg/mL streptomycin. After amplification in T-125 flasks for three passages, lung and skin fibroblasts were seeded at 0.06×10^6 cells/cm².

2.2. *In vitro* imatinib treatment

Pure imatinib mesylate (provided by Novartis Pharma AG, Basel, Switzerland) was resuspended in ddH₂O and added to NRVM or fibroblast cell cultures at concentrations of 0–200 µM for 24 h. Imatinib concentrations were confirmed by HPLC analysis of dosing solutions (data not shown).

2.3. *In vitro* cellular assays

Cellular adenosine triphosphate (ATP) content was determined using a CellTiter–Glo Luminescent Cell Viability Assay® (Promega Corporation, Madison, WI, USA) according to manufacturer's instructions. Cell proliferation was measured by 3-(4,5-dimethylthiazol-2-yl)-5-(3-carboxymethoxyphenyl)-2-(4-sulfophenyl)-2H-tetrazolium inner salt (MTS) reduction using a CellTiter® 96 AQueous Non-Radioactive Cell Proliferation Assay kit (Promega, Madison, WI, USA) according to Malich et al. [13]. Lactate dehydrogenase (LDH) activity was determined with an LDH Cytotoxicity Detection Kit (Roche Molecular Biochemicals, Rotkreuz, Switzerland) according to manufacturer's instructions. Caspase 3/7 activity was shown with a Caspase-Glo® 3/7 Assay (Promega) according to manufacturer's instructions. Cellular ATP:adenosine diphosphate (ADP) ratio was calculated using an ApoSENSOR™ ATP:ADP Ratio Assay kit from BioVision, Inc. (Mountain View, CA, USA) according to Michea et al. [14].

2.4. Real time PCR

XBP-1 and 18S ribosomal RNA probe/primer sets (Applied Biosystems, Foster City, CA, USA) were used for RT-PCR analysis. cDNA was synthesized using the ABI cDNA high-capacity kit (Applied Biosystems). The spliced variants of XBP-1 gene were measured using the following primers and probes: XBP-1 Spliced: Forward 5'-GAGTCCAAGGGGAATGGAG-3', Reverse 5'-TTGTCCAGAATGCCCAAAG-3', Probe 5'-CTGCACTGCTGCGGACT-3'. XBP-1 Unspliced: Forward 5'-GAGTCCAAGGGGAATGGAG-3', Reverse 5'-TTGTCCAGAATGCCCAAAG-3', Probe 5'-TCAGACTACGTGCGCTCT-3'. The relative quantification of gene expression was normalized to 18S rRNA and changes were determined using the standard curve method.

2.5. siRNA knockdown of c-Abl

NRVMs were transfected with Lipofectamine™ 2000 (Invitrogen) according to manufacturer's instructions. GFP-22-modified 3'Alexa 488 siRNA (Qiagen, Valen-

cia, CA, USA) was used as a mismatch control. siRNA against c-Abl was synthesized internally with target sequence TGA TTA TAA CCT AAG ACC CGG. RT-PCR (Applied Biosystems TaqMan® Gene Expression Assay; Rn01436238_g1) and western blot analyses were used to evaluate siRNA knockdown efficiency at the mRNA and protein levels. Cellular ATP, MTS reduction, and caspase 3/7 assays were used to monitor the effect of c-Abl knockdown or response of cells to imatinib under condition of c-Abl knockdown.

2.6. Western blotting

Cardiomyocytes were washed twice in cold phosphate buffered saline (PBS) and lysed in Lysis Buffer (CellLytic M Cell Lysis Reagent, 1/100 vol phosphatase inhibitor cocktail 1, 1/100 vol phosphatase inhibitor cocktail 2, 1/100 vol protease inhibitor cocktail; Sigma–Aldrich Co, St Louis, MO, USA). Lysates were centrifuged for 10 min at $20,000 \times g$ at 4 °C and supernatants were collected and stored at –80 °C. Protein concentration was measured with the Micro BCA Assay Kit (Pierce, Rockford, IL, USA) according to the manufacturer's instructions and quantified with the SpectraMax 250 plate reader (Molecular Devices, Sunnyvale, CA, USA). Protein lysates were prepared in E-PAGE™ Loading Buffer (Invitrogen, Carlsbad, CA, USA) containing Nupage® Sample Reducing Agent (Invitrogen), and run through E-PAGE™ 48.8% gels (Invitrogen). Proteins were then transferred to nitrocellulose membranes using the iBlot® Transfer Stacks (Invitrogen) following manufacturer's instructions. Membranes were blocked for 1 h at room temperature in 50% blocking buffer (LI-COR, Lincoln, NE, USA) in PBS and incubated with the appropriate primary antibodies (overnight at 4 °C) followed by the corresponding secondary antibodies (1 h at room temperature). Blots were then scanned with the Odyssey Infrared Imaging System (LI-COR). Intensity of immunoreactive bands was quantified using Odyssey 2.0 software (LI-COR) and normalized to the reference protein used. The following antibodies and dilutions were used to detect proteins in the western blot assays: c-Abl (Cell Signaling Technology, rabbit; 1:1000 dilution), β-actin (Sigma, mouse; 1:200,000 dilution), goat anti-mouse IgG-IRDye680, and goat anti-rabbit IgG-IRDye800CW (both LI-COR; 1:15,000).

2.7. Animal studies

Imatinib has a long half-life in humans but is rapidly metabolized in mice. While a dose of 400 mg/day is efficacious in leukemia patients [15], much higher doses need to be employed to give efficacy in murine disease models. However, the plasma concentrations leading to efficacy in mice are comparable with the effective concentrations found in plasma of patients [16]. With this insight, in a 4-week og and ip exploratory toxicity study, age-matched wild-type C57BL/6 male mice (RCC and Charles River Laboratories, France) were treated with og or ip vehicle control, og imatinib at 400 mg/kg/day, or ip imatinib at 50 or 200 mg/kg/day for up to 28 days. Oral administration was chosen because it is similar to the method of delivery in humans and ip administration was chosen for ease of comparing data to published preclinical data on imatinib cardiotoxicity.

In another exploratory toxicity study, age-matched wild-type HanRCC:WIST male rats (Research and Consulting Comp, Fullinsdorf, Switzerland) were treated with og vehicle control, og imatinib at 120 mg/kg/day or og imatinib at 180 mg/kg/day for up to 28 days. In a previous internal study, 60 or 180 mg/kg/day og imatinib were shown to induce varying levels of adverse clinical signs in rats, with 180 mg/kg/day considered the maximum tolerated dose for a 4-week study (internal data not published). Studies were performed in conformity with the Swiss Animal Welfare Law and specifically under the Animal License No. 5075 by Cantonal Veterinary Office, Basel-Land.

For the cardiac structure and function study, age-matched wild-type male C57BL/6 mice (Charles River Laboratories, Wilmington, MA, USA) were treated with og vehicle control, og imatinib at 200 mg/kg/day, or feed-administered imatinib at 200 mg/kg/day for up to 35 days. Studies were performed according to the Guide for the Care and Use of Laboratory Animals. Protocols were approved by the Novartis Institutes for BioMedical Research Institutional Animal Care and Use Committee.

2.8. Pathology

Serum creatine kinase activity was measured on a SYNCHRON CX5 delta biochemistry analyzer using the Rosalki method (Beckman Coulter, Fullerton, CA, USA). Plasma cardiac troponin I concentration was measured with a Versamax microplate reader using a High Sensitivity Mouse Cardiac Troponin-I ELISA Kit (Life Diagnostics, West Chester, PA, USA) or a High Sensitivity Rat Cardiac Troponin-I ELISA Kit (Life Diagnostics). Heart, skeletal muscle, and all organs/tissues showing macroscopic abnormalities during necropsy were fixed in neutral phosphate buffered formalin, embedded in paraffin wax, sectioned, stained with hematoxylin and eosin, and examined by light microscopy.

For electron microscopy, heart and skeletal muscle were fixed in 3% glutaraldehyde in 0.1 M cacodylate buffer, pH 7.4 overnight at 4 °C. Postfixation was performed with 1% osmium tetroxide in 0.1 M cacodylate buffer, pH 7.4 for 2 h at 4 °C. Tissues were then dehydrated in graded acetone solutions and embedded in Epon. Semi-thin sections were prepared from tissue blocks, stained with toluidine blue and examined by light microscopy. Ultra-thin sections were prepared from selected samples, counterstained with uranyl acetate and lead citrate and examined by transmission electron microscopy.

Evaluating pathologists were aware of the group assignments of the samples for light and electron microscopy, in accordance with standard best practices in toxicologic pathology used for the evaluation of preclinical safety studies. For light microscopy, tissues were peer reviewed by a second pathologist.

2.9. *In vivo MRI*

Mice were anesthetized with 1–1.5% isoflurane in oxygen and placed in a prone position. Electrocardiogram electrodes were attached to front right and back left paws and a respiratory bellow was placed next to the chest to measure breathing. Multi-slice cardiac cine MRI images were acquired along the principle axes of the heart using a Bruker PharmaScan 4.7T MRI scanner. Average LV myocardial wall thickness measurements were made at the level of the papillary muscle at end-diastole (ED) and end-systole (ES). Left ventricular myocardial volume at ED, and LV chamber volume at ED and ES were calculated by integrating the myocardium and blood pool volume, respectively, over all slices using a truncated cone model. Stroke volume was calculated as LV volume ED – LV volume ES. Percent ejection fraction was calculated as stroke volume/LV volume ED × 100. Left ventricular structure and function were evaluated at baseline (1 week prior to treatment) and after 3 and 5 weeks of treatment.

2.10. *Gene expression profiling*

All GeneChip® experiments were conducted as recommended by the manufacturer of the GeneChip system (Affymetrix Inc, Santa Clara, CA, USA; GeneChip Expression analysis technical manual, 2000). Rat Genome RAE.230.2 and Mouse 430.2 expression probe arrays were used (Affymetrix, Inc). Data were normalized per gene to the mean of the time-matched control group. Gene relevance was considered using the Pearson Correlation, a combination of numerical changes, and the relationship to other modulated genes belonging to a common biological effect.

2.11. *Imatinib plasma levels*

Plasma samples underwent solid-phase extraction on a 96-well 3M Empore C8 plate using an automated Packard Multiprobe pipetting system. Tissue samples were homogenized and homogenates were precipitated using acetonitrile. Determination of imatinib levels in plasma was performed by a solid-phase extraction procedure and analysis by liquid chromatography/tandem mass spectrometry (HPLC/MS/MS) in selected reaction monitoring, positive ion mode using atmospheric pressure chemical ionization (APCI) as an interface.

2.12. *Statistical analysis*

For *in vitro* data, one- or two-way ANOVAs were carried out. The *P* values were compared as either raw *P* values, or adjusted for multiplicity of testing by Dunnett's method. For numerical *in-life* data, Dunnett's test for Student's *t*-test for parametric group comparisons was used. Steel's test of Wilcoxon's test (*U*-test) was used for nonparametric group comparisons [17,18]. For organ weight data, Kolmogorov's test was used to examine the normality of the data and Bartlett's test to examine the homogeneity of variances. Accordingly, either Dunnett's test or Student's *t*-test for parametric group comparisons or Dunn's test or Wilcoxon's test (*U*-test) for nonparametric group comparisons were used. No statistical analysis was performed for nominal or ordinal data (e.g., microscopic examination data). In these cases, the data were compared with data recorded in the reference groups or with historical control data. MRI data were analyzed using two-way repeated measures ANOVA to determine differences in treatment-by-time interaction across groups, and the Holm–Sidak post hoc test was used to determine differences among groups. For non-normally distributed data, a rank transformation was performed prior to the two-

way repeated measures ANOVA. Necropsy data for the cardiac structure and function study were analyzed using a one-way ANOVA, with group differences determined using a Holm–Sidak post hoc test.

3. Results

3.1. *Specificity of imatinib-induced cellular effects*

Imatinib concentration-dependent changes in cytotoxic, apoptotic, or ER stress response markers in NRVMs and three rat-derived fibroblasts of different tissue origins (heart, lung, and skin) were examined following 24 h of imatinib treatment (Fig. 1). Cell viability and cytotoxicity were evaluated using cellular ATP content, MTS reduction, and LDH release; apoptosis and mitochondrial function were evaluated using the ADP:ATP ratio and caspase 3/7 activity; ER stress was evaluated using the XBP1 spliced:unspliced mRNA ratio and CHOP mRNA levels. Data are reported as the concentration of imatinib required to induce a statistically significant change from untreated control cells. No statistically significant differences in cytotoxic, apoptotic, or ER stress responses were observed among NRVMs and different fibroblast cell types following 24 h of imatinib treatment (Fig. 1). Generally, a dose of 10–50 μM imatinib was required to induce ER stress and cell death signal pathways (Fig. 1).

3.2. *Effects of siRNA knockdown of c-Abl*

The levels of c-Abl mRNA expression were similar in NRVMs and fibroblasts; skin and lung fibroblasts expressed roughly an equivalent amount of c-Abl mRNA compared with NRVMs, whereas heart fibroblasts had 30% lower c-Abl mRNA expression (data not shown). The efficiency of c-Abl silencing in NRVMs was examined over 72 h following transfection with 20, 40, or 80 nM of c-Abl siRNA. Both 40 and 80 nM caused a statistically significant (*P* < 0.05) reduction of c-Abl mRNA and protein (Fig. 2). Between 24 and 48 h post-siRNA treatment, c-Abl mRNA expression decreased by 51% (Fig. 2A) and c-Abl protein expression decreased by approximately 70% (Fig. 2B) with 40 or 80 nM c-Abl siRNA. It should be noted that c-Abl silencing in NRVMs did not induce a nonspecific interferon response in transfected cells, demonstrating the specificity of the applied silencing oligonucleotide. Neither the interferon-induced, double-stranded RNA-activated protein kinase gene nor the 2',5'-oligoadenylate synthetase 1 gene were affected by treatment with 40 or 80 nM oligonucleotides. The c-Abl silencing did not change the spontaneous contractility of the cardiomyocytes, nor did it cause changes in ATP homeostasis, apoptosis (caspase 3/7), or ER stress markers (XBP1 and CHOP mRNA) up to 72 h post-transfection compared with GFP controls (data not shown).

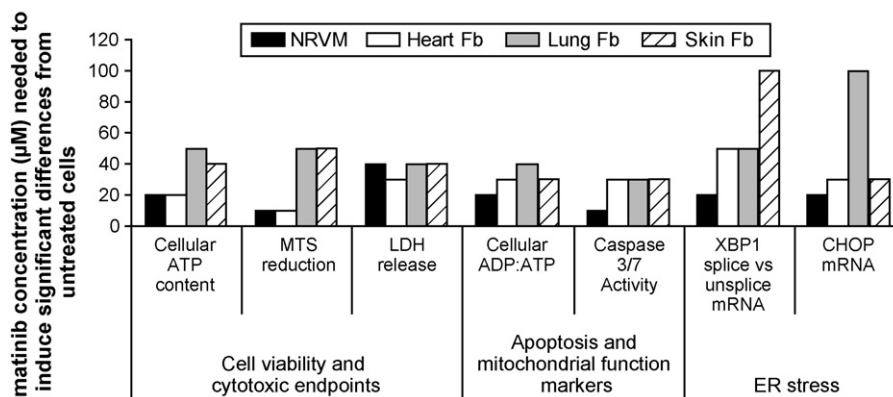


Fig. 1. Effects of 24 h of imatinib treatment with NRVMs or fibroblasts (Fb) on markers of cell viability, cytotoxicity, apoptosis, mitochondrial function and ER stress. Bars denote concentration of imatinib needed to induce significant changes from untreated control cells.

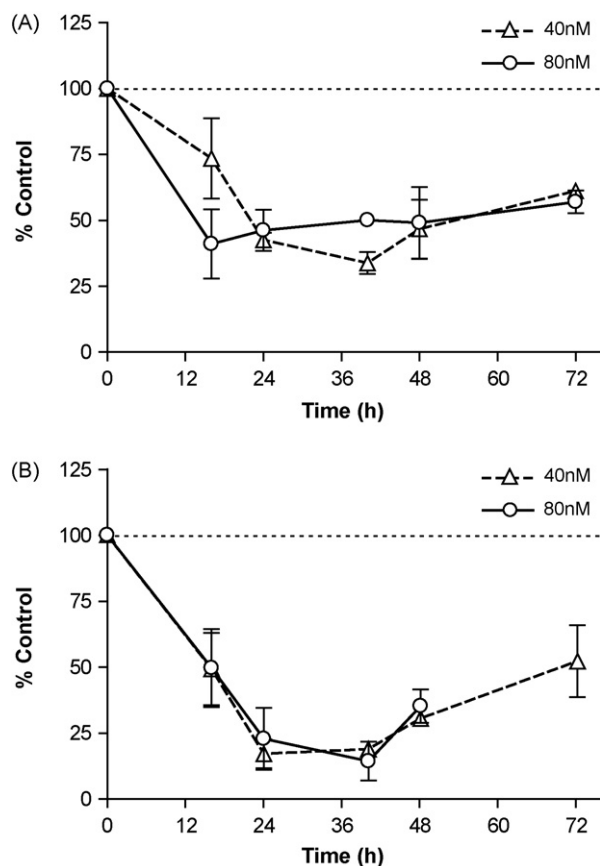


Fig. 2. c-Abl mRNA (A) or protein (B) expression in NRVMs after different times of treatment with 40 and 80 nM siRNA. Data shown as c-Abl expression as percent of untreated control. Both 40 and 80 nM caused a statistically significant ($P < 0.05$) reduction of c-Abl mRNA and protein between 24 and 48 h.

Imatinib-induced cytotoxicity was evaluated in both control (GFP) and c-Abl siRNA-transfected NRVMs between 24 and 48 h post-transfection. In the presence of 30 or 50 μM imatinib there were no statistically significant differences in MTS reduction (Fig. 3A), ATP content (Fig. 3B), or caspase 3/7 activities (Fig. 3C) between cells with and without silenced c-Abl. Thus, a 70% reduction in c-Abl protein expression did not rescue cardiomyocytes from imatinib-induced cytotoxicity.

3.3. Four-week oral exploratory toxicity study in rats

Male HanRCC:WIST rats were given og imatinib at 120 or 180 mg/kg/day. On day 28, both og 120 and 180 mg/kg/day imatinib doses induced slight to moderate increases in serum creatine kinase activity, and og 180 mg/kg/day also induced slight increases in plasma cardiac troponin I concentration in some animals. Both dose- and time-related effects were noted in the heart following microscopic analysis. On day 14, myocardial hypertrophy was minimal to slight in animals treated with imatinib at either dose; incidence and/or severity increased through day 28. On day 28, foci of acute myocardial necrosis were noted in several imatinib-treated rats at both doses. Incidence and severity of inflammatory foci (granulation tissue with or without inflammatory cell infiltration) were increased in imatinib-treated as compared to control-treated rats. No treatment-related lesions were observed in skeletal muscle. By light microscopy, no alterations were seen in toluidine blue-stained heart or skeletal muscle sections.

Electron microscopic examination of heart tissue from rats treated with og 120 mg/kg/day imatinib for 28 days showed normal

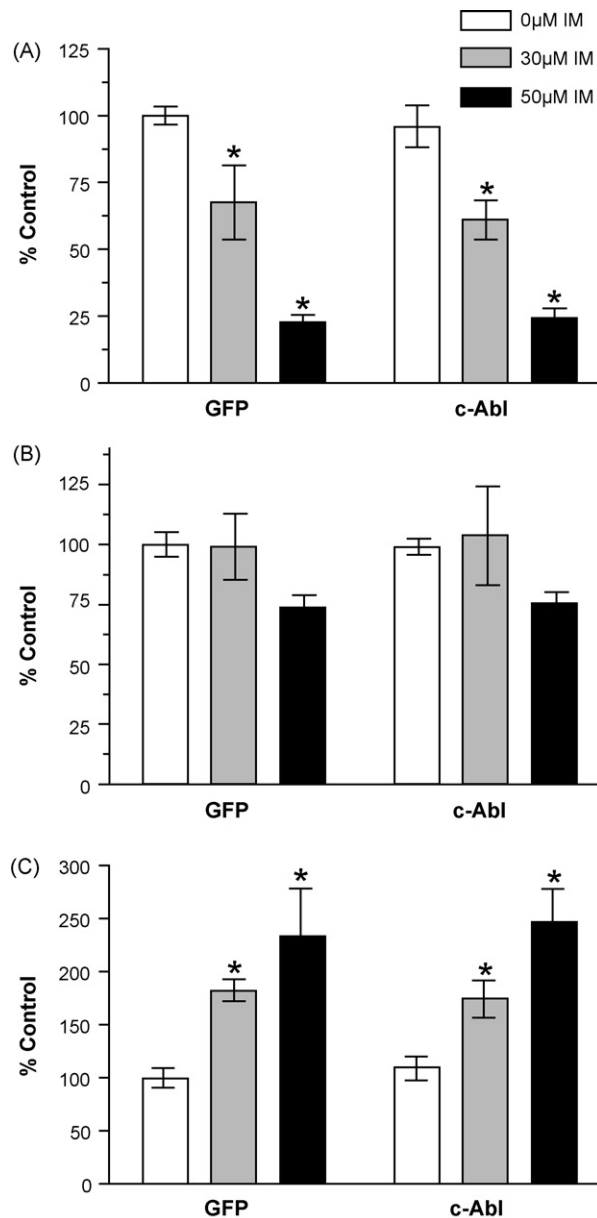


Fig. 3. Effects of imatinib (IM) on MTS reduction (A), ATP contents (B), or caspase 3/7 activity (C) in c-Abl silenced NRVMs (80 nM siRNA 24–48 h post-transfection). Statistically significant changes compared to control were indicated: * $P < 0.001$.

morphology of cellular organelles with only very rare occurrence of single myeloid bodies in a few capillary endothelial cells. All other cellular organelles showed the same morphology and distribution as in corresponding control-treated animals (Fig. 4A). Heart tissue from rats treated with og 180 mg/kg/day imatinib for 28 days showed electron-dense cytoplasmic inclusion bodies often containing concentrically arranged lamellae (myeloid bodies) in Schwann cells (Fig. 4B), capillaries, endothelial cells, and macrophages. Additionally, lysosomes containing electron-opaque granular material were observed in some myocytes.

Electron microscopic examination of skeletal muscle tissue from rats treated with og 180 mg/kg/day imatinib for 28 days demonstrated electron-dense cytoplasmic inclusion bodies in capillary endothelial cells (Fig. 4C), macrophages, and electron-dense cytoplasmic inclusion bodies (myeloid bodies). One animal had a focal increase of cytolysosomes containing mitochondria in variable stages of digestion and other cytoplasmic fragments (Fig. 4D).

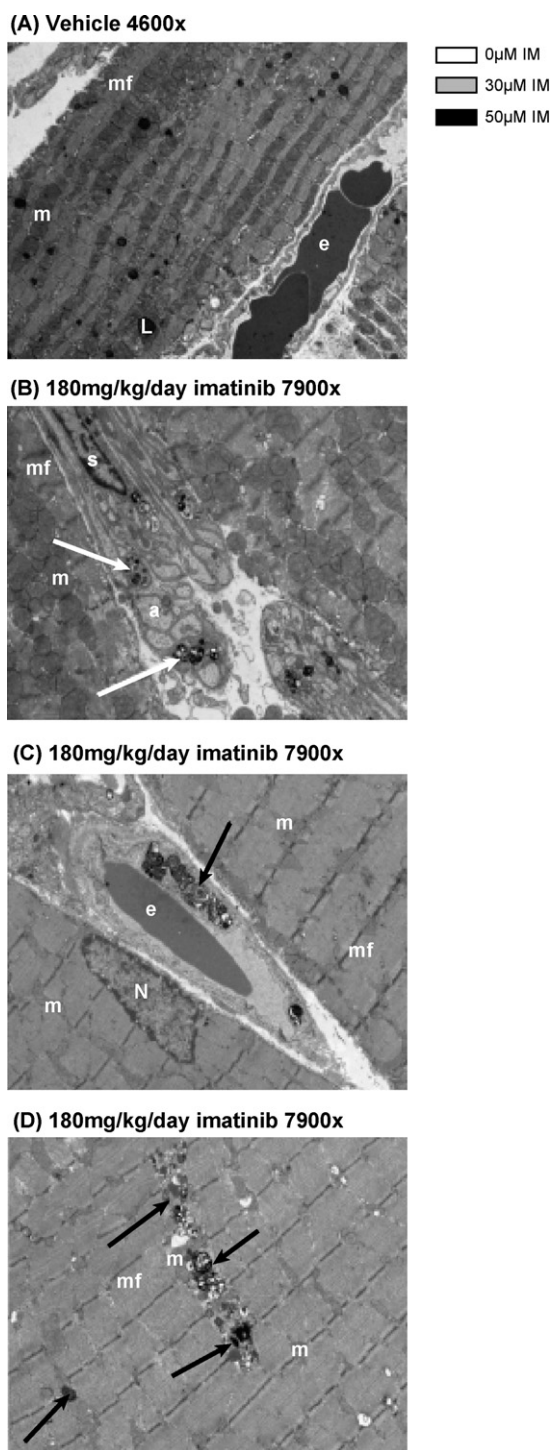


Fig. 4. Electron micrographs of ventricular myocardium (A and B) or skeletal muscle (C and D) from rats treated for 28 days as labeled. Note the lipid droplets (L) in the cytoplasm often located between the ends of mitochondria. Note the myeloid bodies in the cytoplasm of the Schwann cell (B, white arrows) and endothelial cells (C, black arrow). Note the cytolysosomes (black arrows) in the skeletal muscle fibers located between the mitochondria (D, lower right). Key: a, axon; m, mitochondria; e, erythrocyte; mf, myofibrils; N, nucleus of skeletal muscle cell; S, Schwann cell. Magnification noted on each image.

Skeletal muscle from rats treated with og 120 mg/kg/day imatinib for 28 days displayed normal morphology of cellular organelles with only very rare occurrence of single myeloid bodies in a few endothelial cells of capillaries and between mitochondria of muscle fibers.

Gene and protein expression profiling resulted in heart tissue that correlated with histopathological observations and indicated a clear dose and time-dependent response after treatment with imatinib (Table 1). The gene signature pointed to an alteration in the expression of inflammatory/stress-related genes in a time- and dose-dependent manner. Additional gene modulation was related to hypertrophic signaling, vascular remodeling, and vascular tone. No direct effect on genes related to mitochondrial structure and ATP pool or ER stress could be observed. The sporadic alterations in few oxidative stress genes pointed to a secondary event linked to the observed hypertrophy.

Exposure to imatinib dose-proportionally increased from og 120 to 180 mg/kg/day. T_{max} was shortened from 3 h at og 120 mg/kg/day to 1 h at og 180 mg/kg/day (Table 2).

3.4. Four-week oral and intraperitoneal exploratory toxicity studies in mice

C57BL/6 mice were treated with og imatinib at 400 mg/kg/day, or ip imatinib at 50 or 200 mg/kg/day for up to 28 days. Two mice were found dead 24 h after the second administration of ip 200 mg/kg/day imatinib; the remaining mice in this group were sacrificed on day 3. Since ip imatinib administration at 200 mg/kg showed severe local toxicity, this group of mice was not further taken into consideration for the evaluations. Mice receiving ip 50 mg/kg/day imatinib were sacrificed following the 22nd dose due to local toxicity at the ip injection site. Lesions related to local toxicity were seen in abdominal organs of mice receiving ip imatinib. No clear test item-related changes were observed by clinical pathology in mice administered imatinib og 400 mg/kg or ip 50 mg/kg.

No light or electron microscopic treatment-related lesions in heart or skeletal muscle were noted with og or ip imatinib. However, electron microscopy of heart tissue from control and ip 50 mg/kg imatinib-treated animals occasionally showed a few swollen mitochondria, some vacuoles containing membrane whorls (myelin figures), dilated sarcoplasmic reticulum membranes, and lysosomes containing electron-dense granular material (Fig. 5A–C). All of these alterations were seen at similar levels on controls and imatinib-treated animals and were considered to be fixation artifacts.

For the ip route of administration, gene and protein expression profiling demonstrated induction of different transcriptional changes related to the acute phase response, immune stress response, degeneration/regeneration, and oxidative stress. These changes were the consequence of the local toxicity observed when imatinib was administered via the ip route. For the oral route of administration, the transcriptional changes induced by imatinib were very minimal and not toxicologically relevant.

For the ip route, C_{max} under-proportionally increased between 50 and 200 mg/kg/day whereas AUC_{0-24h} proportionally increased between both doses (Table 3). T_{max} was much later for the 200 mg/kg/day dose, potentially related to intraperitoneal lesions and/or fast metabolism of the parent compound. Imatinib concentration in the heart over-proportionally increased between 50 and 200 mg/kg/day.

3.5. Cardiac function and structure in mice treated with imatinib for 5 weeks

Several markers of cardiac structure or function were measured in mice over 35 days of imatinib treatment, none of which showed significant differences among vehicle- or imatinib-treated (og or oral in feed 200 mg/kg/day) animals. *In vivo* MRI was used for measurements, as it is more sensitive for cardiac assessment than echocardiography [19]. MRI-derived LV myocardial volume revealed changes within each group over time; however, there

Table 1
Fold change in gene expression after imatinib treatment of heart tissue.

Gene description	120 mg/kg/day ^a for 28 days	180 mg/kg/day ^a for 28 days
Inflammatory/stress		
Secreted phosphoprotein 1 (Spp1)	8.3	27.3
Glycoprotein (transmembrane) nmb	2.2	13.8
Pancreatitis-associated protein	5.4	11.8
Metallothionein 1a	1.5	2.8
Lipocalin 2	2.3	2.6
Genes related to hypertrophic cardiomyopathy		
Myosin, heavy polypeptide 7, cardiac muscle	−1.0	2.4
Sarcolipin	2.2	2.0
Actin, alpha 1	1.2	1.6
Tropomyosin 3, gamma	1.3	1.5
Vascular remodeling		
Angiopietin 2	2.6	2.6
von Willebrand factor	1.6	2.3
FMS-like tyrosine kinase 1	1.3	1.7
Endoglin	1.3	1.6
Vascular tone		
Natriuretic peptide precursor type A	2.4	4.1
Adrenomedullin	1.6	2.2
Angiotensin I converting enzyme	1.6	2
Natriuretic peptide precursor type B	1.3	1.9
Oxidative stress (oxidant/anti-oxidant)		
Aconitase 2, mitochondrial	1.0	1.0
Catalase	−1.1	1.1
Glutathione peroxidase 1	1.1	1.1
Superoxide dismutase 1	1.0	1.0
ATX1 (anti-oxidant protein 1) homolog 1	1.0	1.0
Peroxiredoxin 1	1.0	1.1
Thioredoxin reductase 1	1.1	1.1
Mitochondrial oxidative phosphorylation		
ATP synthase, H+ transporting, F0 complex	1.0	1.0
ATP synthase, H+ transporting, F1 complex	1.0	1.0
Cytochrome c oxidase subunit VIII-H	1.0	1.0
Cytochrome c oxidase, subunit Va	1.0	1.0
NADH dehydrogenase 1 beta 3	1.1	1.1
NADH dehydrogenase 1 alpha/beta 1	1.0	1.0
ER stress		
Homocysteine-inducible, endoplasmic reticulum stress-inducible, ubiquitin-like domain member 1	1.0	1.2
HERPUD family member 2	−1.1	1.0

^a Fold change: Data were normalized per gene to the mean of the control group.

were no differences among the groups at specific time points. Thus, imatinib treatment had no effect on absolute or normalized LV mass (Fig. 6). These MRI results are supported by the necropsy results, which also showed no significant differences in absolute or normalized heart mass among the groups. Other parameters which were comparable between vehicle- and imatinib-treated mice included: average body weight, food consumption, ejection fraction, heart mass at necropsy, tibia length at necropsy, LV myocardial wall thickness, and LV end-diastolic chamber volume.

Table 2
Toxicokinetic parameters of imatinib in rat plasma and heart at end of treatment.

	og 120 mg/kg/day imatinib	og 180 mg/kg/day imatinib
Plasma		
Mean T_{max} (h)	3	1
Mean C_{max} (ng/mL)	7,430	9,420
Mean AUC _{0–24h} (ng · h/mL)	115,000	146,000
Heart		
Mean C_{max} (ng/mL)	35,700	47,700

AUC, area under the concentration–time curve; C_{max} , maximal concentration for each treatment group; og, oral gavage; T_{max} , time to maximal plasma concentration for each treatment group.

As with the mice and rat exploratory toxicity studies, plasma C_{max} and AUC_{0–24h} levels were similar or above the levels found in patients receiving therapeutic levels of imatinib (Table 4). In a phase I trial of CML patients, patient C_{max} with 400 mg twice daily imatinib (total of 800 mg) was 2315–3063 ng/mL and AUC was 68,400 ng · h/mL [20].

Table 3
Toxicokinetic parameters of imatinib in mouse plasma and heart at the end of treatment.

	Oral gavage (og)	Intraperitoneal (ip)	
	400 mg/kg/day	50 mg/kg/day	200 mg/kg/day
Plasma			
Mean T_{max} (h)	0.5	0.2	3.0
Mean C_{max} (ng/mL)	38,200	12,000	19,000
Mean AUC _{0–24h} (ng · h/mL)	244,000	20,700	94,100
Heart			
Mean C_{max} (ng/mL)	41,200	32,700	7,840

AUC, area under the concentration–time curve; C_{max} , maximal concentration for each treatment group; og, oral gavage; T_{max} , time to maximal plasma concentration for each treatment group.

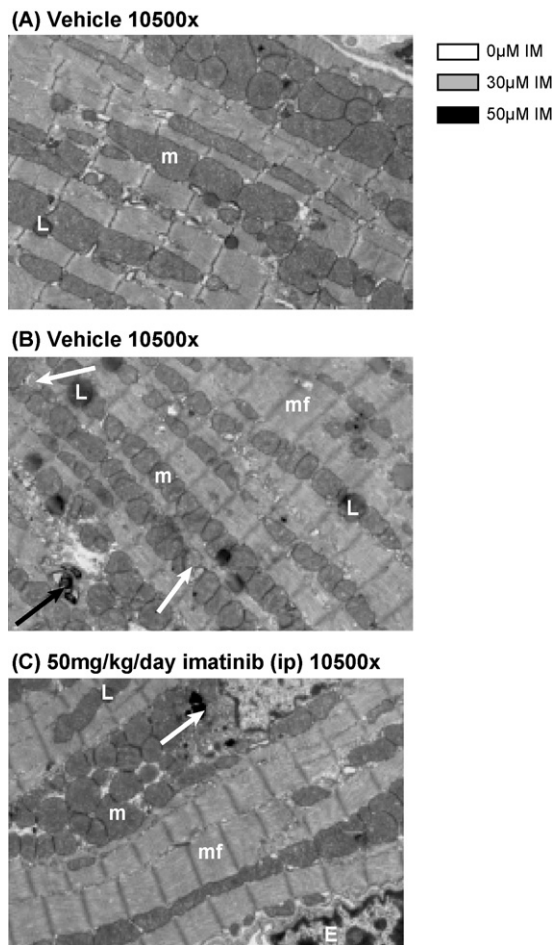


Fig. 5. Electron micrographs of ventricular myocardium from mice treated for 28 days as labeled. Note the lipid droplets (L) in the cytoplasm often located between the ends of mitochondria. In some control samples (image B) there were vacuoles containing membrane whorls (B, black arrow) and swollen mitochondria (B, white arrows). Note the lysosomes with electron-dense granular material (C, white arrow). Key: m, mitochondria; mf, myofibrils; E, nucleus of endothelial cell. Magnification noted on each image.

4. Discussion

This study demonstrates that cytotoxic concentrations of imatinib (10–50 μM) are required to trigger activation of the ER stress response, collapse of the mitochondrial membrane potential, reduction in cellular ATP content, and cell death in NRVMs. In accordance with previously published data [20–22], imatinib had an IC_{50} of approximately 0.5 μM in the Ba/F3-Bcr-Abl murine hematopoietic cell model used in this study, with nearly complete inhibition of BCR-ABL activity at 1 μM . Assuming similar effects on NRVMs, these results suggest saturated inhibition of c-Abl kinase in the 10–50 μM concentration range. This implies that further increases in the dose of imatinib above 10 μM should not significantly increase c-Abl-mediated effects of imatinib in NRVMs. However, a clear

Table 4
Pharmacokinetic parameters of imatinib in mouse plasma at the end of treatment.

	og 200 mg/kg/day	Oral in feed 200 mg/kg/day
Plasma		
Mean C_{max} (ng/mL)	31,500	4,220
Mean $\text{AUC}_{0-24\text{h}}$ (ng · h/mL)	93,500	68,300

AUC, area under the concentration–time curve; C_{max} , maximal concentration for each treatment group; og, oral gavage.

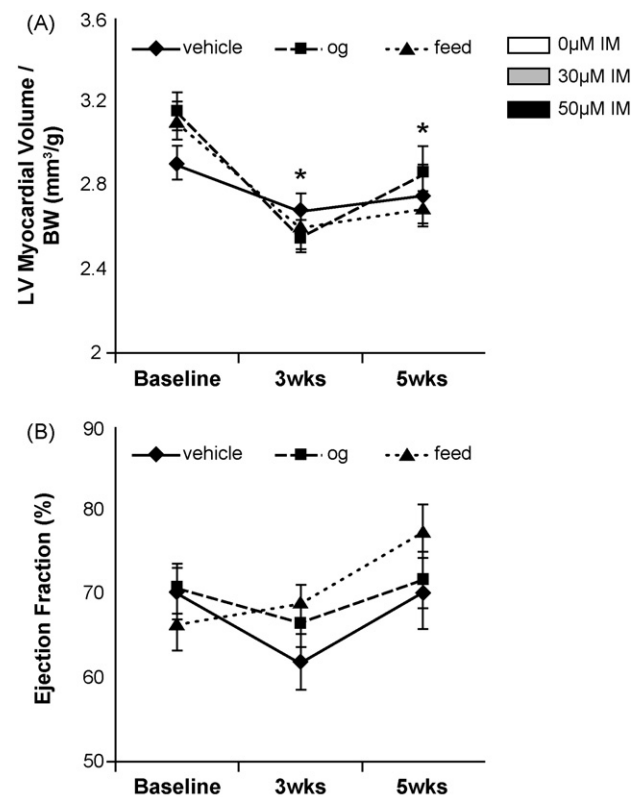


Fig. 6. Longitudinal results from *in vivo* cardiac magnetic resonance imaging in C57Bl/6 mice treated for up to 5 weeks with vehicle by og, or 200 mg/kg/day imatinib by og or through feed. (A) Left ventricular myocardial volume, normalized by body weight (BW), as a measure of hypertrophy. (B) Left ventricular ejection fraction, as a measure of systolic function. No significant treatment effects were observed in these endpoints at all time points. * $P < 0.01$ vs baseline.

dose–response relationship above 10 μM for cytotoxicity, ER stress response, and cell death signaling pathways was observed, suggesting that these were c-Abl-independent effects. Furthermore, the post-transcriptional silencing of c-Abl through siRNA had no effect on the spontaneous beating frequency of cardiomyocytes, and did not induce cytotoxicity, apoptosis, mitochondrial dysfunction, or ER stress response in NRVMs, demonstrating that c-Abl is not likely to play a major role in these processes in heart tissue. Additionally, the 70% reduction of c-Abl protein achieved by c-Abl gene silencing did not rescue NRVMs from imatinib-induced cytotoxicity and had no effect on imatinib-induced beating frequencies, suggesting that imatinib-related cytotoxicity is not related to the drug’s inhibition of c-ABL.

Imatinib-induced increase in caspase 3/7 activation was observed in heart, lung, and skin fibroblasts, correlating with increases in both ADP:ATP ratio and ER stress markers. Caspase 3/7 activation is a downstream event of the mitochondrial cytochrome c release and is an established marker for the execution of apoptosis. Additionally, mRNA expression of two ER stress markers, XBP1 and CHOP, was statistically significantly increased after imatinib treatment in the cytotoxic concentration range in all heart, lung and skin fibroblasts. Thus, imatinib does not appear to specifically affect apoptosis pathways in cardiomyocytes because similar effects were observed in fibroblasts from different organs. Furthermore, c-Abl mRNA expression levels were generally similar across cell types. Although heart fibroblasts had a 30% lower expression compared with NRVMs or lung or skin fibroblasts, this difference seems unlikely to result in different toxic responses to imatinib.

Blood concentrations of imatinib achieved in rats were comparable with or higher than those reported for humans at therapeutic

doses; in a phase I trial human steady state imatinib C_{\max} (mean \pm standard deviation) was 2596.0 ± 786.7 ng/mL for 400 mg once daily dosing and 3701.8 ± 1433.5 ng/mL for 400 mg twice daily [23]. Repeated administration of imatinib by oral gavage at 120 or 180 mg/kg/day to rats for 14 or 28 days to rats was tolerated without mortality or treatment-related clinical signs. However, imatinib treatment did result in dose- and time-dependent morphologic cardiac effects. Specifically, there was evidence in some animals of increased heart weight, increases in creatine kinase and troponin I, myocardial hypertrophy, and occasionally foci myocardial necrosis. These effects were similar to those reported in the 2-year rat carcinogenicity study and are appropriately addressed in the product label [7]. There are several concomitant pathologies (such as an increase in alveolar macrophages, nephrotoxicity, and anemia) that may be contributing to the myocardial hypertrophy seen in rats after long-term or high-dose imatinib therapy by increasing the cardiac workload. Electron microscopy revealed no effects on organelles of cardiomyocytes, but did reveal the presence of myeloid bodies in endothelial cells, Schwann cells, and macrophages with imatinib treatment at og 180 mg/kg/day. Importantly, these microscopic alterations were not specific to heart muscle, as they were also seen in electron microscopy of skeletal muscle from imatinib-treated rats. The only imatinib-specific adverse effects of og 120 mg/kg/day imatinib visible by electron microscopy were rare occurrences of single myeloid bodies in endothelial cells.

No treatment-related alterations in heart or skeletal muscle were observed in this study, and there were no significant changes in heart weight. Imatinib at og 400 mg/kg/day or ip 50 mg/kg/day was generally clinically well tolerated up to 28 days. Mice given ip administration at 50 mg/kg/day showed signs of local abdominal toxicity, but light and electron microscopic evaluations of the heart showed no treatment-related findings. The swollen mitochondria and myelin figures seen by electron microscopy in samples from some control mice or mice treated with ip 50 mg/kg/day imatinib were considered to be fixation artifacts. Effectively, immersion fixation of small tissue blocks can easily cause artifacts which may be misinterpreted as treatment-related alterations [24]. Imatinib administered ip at 200 mg/kg/day imatinib was not well tolerated due to local toxicity related to the route of administration and led to death in two of five mice. Five weeks of oral (gavage or feed) 200 mg/kg/day imatinib treatment in mice did not induce any changes in LV structure or function indicative of overt cardiovascular pathology or heart failure.

Several publications have examined the possibility of imatinib-induced cardiotoxicity with conflicting conclusions. Will et al. found that imatinib induced no mitochondrial effects at therapeutic concentrations in rat heart mitochondria [25]. Kerkela et al. reported clinical findings of LV contractile dysfunction accompanied by signs and symptoms of heart failure in 10 human patients following imatinib therapy [11]. The authors concluded that cardiac dysfunction was caused by imatinib therapy, as patients had no predisposing conditions. The clinical observations described were supported by echocardiogram findings in mice treated with imatinib for 5 weeks at dose of 200 mg/kg/day, showing reduced ejection fraction and moderate LV dilation. The authors concluded from these *in vivo* mouse data, as well as an *in vitro* NRVM study, that imatinib specifically induced cardiomyocyte cell death by triggering ER stress and collapsed mitochondrial membrane potential. Their *in vitro* study used retroviral gene transfer, with above 90% of cells being efficiently infected, of an imatinib-resistant mutant c-Abl into NRVMs. The gene transfer appeared to alleviate imatinib-induced cell death and it was concluded that the observed imatinib-induced cardiotoxicity was mediated through direct interactions of imatinib with c-Abl [11]. Retroviral gene transfer is known to be effective in dividing cells only [26]. In our

hands, NRVMs had a maximum replication rate of 7% of the population only as measured by BrdU incorporation (data not shown). In another study, Fernandez et al. made a chemical modification to imatinib that hampered *BCR-ABL* inhibition while maintaining c-Kit inhibition [27]. The authors showed that hampering *BCR-ABL* inhibition led to less cardiotoxicity in mice at doses exceeding the therapeutic range. However, the modified imatinib used in that study also inhibited JNK1/2 activation. JNK activation has been associated with cardiomyocyte apoptosis via collapse of the mitochondrial membrane potential and release of cytochrome c [28]. Thus, results from this study on the specific effect of *BCR-ABL* inhibition on imatinib-induced cardiotoxicity are difficult to interpret. Freebern et al. found that imatinib at pharmacologically relevant concentrations significantly affected mitochondrial membrane potential, cell viability, apoptosis, and cellular ultrastructure in primary rat cardiomyocytes [29]. Thus, there has been no clear consensus in the literature concerning the imatinib-induced pre-clinical cardiotoxicity.

Preclinical studies investigating the potential of imatinib-induced cardiotoxicity, including the studies described herein, typically lasted several weeks. However, human patients may receive imatinib for several years. Thus, it is important to take the information gathered from preclinical studies, and also specifically examine more long-term clinical results related to cardiotoxicity. Atallah et al. reviewed all reported serious cardiac adverse events occurring in patients on clinical trials involving imatinib [30]. Among 1276 patients enrolled, 22 (1.7%, median age 70) were identified as having symptoms that could be attributed to systolic heart failure, 8 (0.6%) of which were reported as possibly or probably related to imatinib. Of these 22, 18 had previous medical conditions predisposing them to cardiac failure, including congestive heart failure, diabetes mellitus, hypertension, coronary artery disease, arrhythmia, and cardiomyopathy. Thus, imatinib-associated heart failure was shown to be uncommon in this large meta-analysis, and primarily occurred in elderly patients with pre-existing cardiac dysfunction [30]. Similarly, Verweij et al. examined 946 patients (median time on imatinib, 24 months) enrolled in a gastrointestinal stromal tumor (GIST) clinical trial, and found that only 2 (0.2%) patients had a cardiotoxic effect possibly related to imatinib [31]. Finally, Ribeiro et al. studied 103 consecutive patients with CML on treatment with imatinib and 57 with chronic myeloproliferative disorders not treated with imatinib [32]. They found no statistically significant difference regarding cardiac symptoms and signs, B-type natriuretic peptide (BNP) levels, and echocardiographic measurements for imatinib and control groups, except for peripheral edema, which was more frequent in the imatinib group. Thus, it appears imatinib is not the cause of systematic deterioration of cardiac function, but rather rare isolated cases of potential cardiotoxicity.

In the present study, imatinib-induced cardiotoxic effects typically occurred *in vitro* or in rats at concentrations higher than that needed for clinical efficacy (5 μ M). Additionally, treatment with imatinib in mice or rats did not induce transcriptomic changes related to direct oxidative stress, mitochondrial integrity, or the ATP pool. Overall, treatment with imatinib did not induce cardiovascular pathology or heart failure in mice. Multiple organ toxicities likely contributed to the myocardial hypertrophy which occurred only in rats treated with high doses of imatinib. This preclinical study affirms the very favorable risk/benefit ratio of imatinib for the treatment of life-threatening malignant disorders.

Conflict of interest statement

All authors are employees of Novartis Pharma AG or Novartis Pharmaceuticals Corporation.

Acknowledgements

Financial support for medical editorial assistance was provided by Novartis Pharmaceuticals Corporation.

Contributions. The authors would like to thank the following persons for their valuable scientific and technical contributions: Yun Jiang, Jonathan Moggs, Enrico Funhoff, Axel Vicart, Sabine Ackerknecht, Virginie Riebel, Magalie Marcelin, Manuella Goetschi, and Brigitte Greiner. We thank Stacey Rose, PhD (Articulate Science) for medical editorial assistance with this manuscript.

References

- [1] Rowley JD. Letter: a new consistent chromosomal abnormality in chronic myelogenous leukaemia identified by quinacrine fluorescence and Giemsa staining. *Nature* 1973;243:290–3.
- [2] Shtivelman E, Lifshitz B, Gale RP, Canaani E. Fused transcript of abl and bcr genes in chronic myelogenous leukaemia. *Nature* 1985;315:550–4.
- [3] Sawyers CL. Chronic myeloid leukemia. *N Engl J Med* 1999;340:1330–40.
- [4] Faderl S, Talpaz M, Estrov Z, O'Brien S, Kurzrock R, Kantarjian HM. The biology of chronic myeloid leukemia. *N Engl J Med* 1999;341:164–72.
- [5] Day E, Waters B, Spiegel K, et al. Inhibition of collagen-induced discoidin domain receptor 1 and 2 activation by imatinib, nilotinib and dasatinib. *Eur J Pharmacol* 2008;599:44–53.
- [6] Weisberg E, Manley PW, Cowan-Jacob SW, Hochhaus A, Griffin JD. Second generation inhibitors of BCR-ABL for the treatment of imatinib-resistant chronic myeloid leukaemia. *Nat Rev Cancer* 2007;7:345–56.
- [7] Gleevec (imatinib) [package insert]. East Hanover, NJ: Novartis Pharmaceuticals Corporation; 2008.
- [8] O'Brien SG, Guilhot F, Larson RA, et al. Imatinib compared with interferon and low-dose cytarabine for newly diagnosed chronic-phase chronic myeloid leukemia. *N Engl J Med* 2003;348:994–1004.
- [9] Druker BJ, Guilhot F, O'Brien SG, et al. Five-year follow-up of patients receiving imatinib for chronic myeloid leukemia. *N Engl J Med* 2006;355:2408–17.
- [10] O'Brien SG, Guilhot F, Goldman JM, et al. International randomized study of interferon versus ST1571 (IRIS) 7-year follow-up: sustained survival, low rate of transformation and increased rate of major molecular response (MMR) in patients (pts) with newly diagnosed chronic myeloid leukemia in chronic phase (CML-CP) treated with imatinib (IM). *Blood* 2008;112:76.
- [11] Kerkela R, Grazette L, Yacobi R, et al. Cardiotoxicity of the cancer therapeutic agent imatinib mesylate. *Nat Med* 2006;12:908–16.
- [12] Toraason M, Luken ME, Breitenstein M, Krueger JA, Biagini RE. Comparative toxicity of allylamine and acrolein in cultured myocytes and fibroblasts from neonatal rat heart. *Toxicology* 1989;56:107–17.
- [13] Malich G, Markovic B, Winder C. The sensitivity and specificity of the MTS tetrazolium assay for detecting the in vitro cytotoxicity of 20 chemicals using human cell lines. *Toxicology* 1997;124:179–92.
- [14] Michea L, Combs C, Andrews P, Dmitrieva N, Burg MB. Mitochondrial dysfunction is an early event in high-NaCl-induced apoptosis of mIMCD3 cells. *Am J Physiol Renal Physiol* 2002;282:F981–990.
- [15] Larson RA, Druker BJ, Guilhot FA, et al. Imatinib pharmacokinetics and its correlation with response and safety in chronic phase chronic myeloid leukemia: a subanalysis of the IRIS study. *Blood* 2008;111:4022–8.
- [16] Druker BJ, Talpaz M, Resta DJ, et al. Efficacy and safety of a specific inhibitor of the BCR-ABL tyrosine kinase in chronic myeloid leukemia. *N Engl J Med* 2001;344:1031–7.
- [17] Miller RG. Simultaneous statistical inference. 2nd ed. New York, NY: Springer; 1981.
- [18] Zar JH. Biostatistical analyses. 2nd ed. Englewood Cliffs, NJ: Prentice-Hall; 1984.
- [19] Grothues F, Smith GC, Moon JC, et al. Comparison of interstudy reproducibility of cardiovascular magnetic resonance with two-dimensional echocardiography in normal subjects and in patients with heart failure or left ventricular hypertrophy. *Am J Cardiol* 2002;90:29–34.
- [20] Druker BJ, Tamura S, Buchdunger E, et al. Effects of a selective inhibitor of the Abl tyrosine kinase on the growth of Bcr-Abl positive cells. *Nat Med* 1996;2:561–6.
- [21] Deininger M, Buchdunger E, Druker BJ. The development of imatinib as a therapeutic agent for chronic myeloid leukemia. *Blood* 2005;105:2640–53.
- [22] Manley PW, Cowan-Jacob SW, Mestan J. Advances in the structural biology, design and clinical development of Bcr-Abl kinase inhibitors for the treatment of chronic myeloid leukaemia. *Biochim Biophys Acta* 2005;1754:3–13.
- [23] Peng B, Hayes M, Resta D, et al. Pharmacokinetics and pharmacodynamics of imatinib in a phase I trial with chronic myeloid leukemia patients. *J Clin Oncol* 2004;22:935–42.
- [24] Ultrastructural pathology of the cell. A text atlas of physiological and pathological alterations in cell fine structure. London/Boston: Butterworths; 1975.
- [25] Will Y, Dykens JA, Nadanaciva S, et al. Effect of the multitargeted tyrosine kinase inhibitors imatinib, dasatinib, sunitinib, and sorafenib on mitochondrial function in isolated rat heart mitochondria and H9c2 cells. *Toxicol Sci* 2008;106:153–61.
- [26] Miller DG, Adam MA, Miller AD. Gene transfer by retrovirus vectors occurs only in cells that are actively replicating at the time of infection. *Mol Cell Biol* 1990;10:4239–42.
- [27] Fernandez A, Sanguino A, Peng Z, et al. An anticancer C-Kit kinase inhibitor is reengineered to make it more active and less cardiotoxic. *J Clin Invest* 2007;117:4044–54.
- [28] Baines CP, Molkenin JD. STRESS signaling pathways that modulate cardiac myocyte apoptosis. *J Mol Cell Cardiol* 2005;38:47–62.
- [29] Freebern WJ, Fang HS, Slade MD, et al. In vitro cardiotoxicity potential comparative assessments of chronic myelogenous leukemia tyrosine kinase inhibitor therapies: dasatinib, imatinib and nilotinib. *Blood* 2007;110:4582.
- [30] Atallah E, Durand JB, Kantarjian H, Cortes J. Congestive heart failure is a rare event in patients receiving imatinib therapy. *Blood* 2007;110:1233–7.
- [31] Verweij J, Casali PG, Kotasek D, et al. Imatinib does not induce cardiac left ventricular failure in gastrointestinal stromal tumours patients: analysis of EORTC-ISG-AGITG study 62005. *Eur J Cancer* 2007;43:974–8.
- [32] Ribeiro AL, Marcolino MS, Bittencourt HN, et al. An evaluation of the cardiotoxicity of imatinib mesylate. *Leuk Res* 2008;32:1809–14.